ANALYTIC THEORY FOR THE YARKOVSKY–O'KEEFE–RADZIEVSKI–PADDACK EFFECT ON OBLIQUITY

DAVID NESVORNÝ[1] AND DAVID VOKROUHLICKÝ[2]

[1] Department of Space Studies, Southwest Research Institute, 1050 Walnut St., Suite 300, Boulder, CO 80302, USA
[2] Institute of Astronomy, Charles University, V Holešovičkách 2, CZ-18000, Prague 8, Czech Republic

ABSTRACT

The Yarkovsky–O'Keefe–Radzievski–Paddack (YORP) effect is a thermal radiation torque that causes small objects to speed up or slow down their rotation and modify their spin vector orientation. This effect has important implications for spin dynamics of diameter $D \lesssim 50$ km asteroids. In our previous work we developed an analytic theory for the component of the YORP torque that affects the spin rate. Here we extend these calculations to determine the effect of the YORP torque on obliquity. Our theory is limited to objects with near-spherical shapes. Two limiting cases are studied: (1) immediate emission of the thermal energy that occurs for surface thermal conductivity $K = 0$; (2) the effects of $K \neq 0$ in the limit of small temporal variations of the surface temperature. We use the linearized heat transport equation to model (2). The results include explicit scaling of the YORP torque on obliquity with physical and dynamical parameters such as the thermal conductivity and spin rate. The dependence of torques on the obliquity is given as series of the Legendre polynomials. Comparisons show excellent agreement of the analytic results with the numerically calculated YORP torques for objects such as asteroids 1998 KY$_{26}$ and (66391) 1999 KW$_4$. We suggest that an important fraction of main belt asteroids may have specific obliquity values (generalized Slivan states) arising from the roots of the Legendre polynomials.

Key words: minor planets, asteroids

Online-only material: machine-readable and VO tables

1. INTRODUCTION

The thermal Yarkovsky–O'Keefe–Radzievski–Paddack (YORP) torque on an object is

$$\boldsymbol{\tau} = -\frac{2}{3}\frac{\varepsilon_t \sigma}{v_c} \int_S dS(\boldsymbol{r} \times \boldsymbol{n})T_s^4, \qquad (1)$$

where ε_t is the object's material emissivity in thermal wavelengths (assumed here to be constant over the surface), $v_c = 2.997,92458 \times 10^8$ m s^{-1} is the speed of light, $\sigma = 5.6704 \times 10^{-8}$ W m^{-2} K^{-4} is the Stefan–Boltzmann constant, and T_s is the surface temperature. Vector $\boldsymbol{n}$ is a unit vector pointing from the surface element dS in the normal direction. Vector $\boldsymbol{r}$ connects an arbitrary point in the object, to be conveniently chosen to coincide with its center of mass (COM), to the surface element dS.

The two important components of the YORP torque are $\tau_s = \tau_z$, where τ_z is the z component of vector $\boldsymbol{\tau}$ in the body frame, and

$$\tau_\epsilon = \frac{1}{\sin \epsilon}[(\boldsymbol{\tau} \cdot \boldsymbol{s})\cos \epsilon - \boldsymbol{\tau} \cdot \boldsymbol{o}], \qquad (2)$$

where $\boldsymbol{s} = (0, 0, 1)^{\mathrm{T}}$ is a unit spin vector assumed here to be aligned with the z axis in the body frame, $\boldsymbol{o}$ is a unit vector normal to the orbital plane and the index T denotes the transposed matrix (Rubincam 2000; Vokrouhlický & Čapek 2002). Assuming the principal axis rotation, these two torque components control the behavior of the rotation speed, $\omega > 0$, and obliquity, ϵ, according to $d\omega/dt = \bar{\tau}_s/C$, $d\epsilon/dt = \bar{\tau}_\epsilon/C\omega$ (C denotes the principal moment of inertia; Rubincam 2000).

We limit the analysis in this paper to the Keplerian orbital motion of a small body around the Sun and its rotation around the axis of maximum inertia. To calculate the mean YORP torque, which controls the long-term behavior of the spin vector, we average $\boldsymbol{\tau}$ over the spin and orbit periods of the small object. The mean YORP torques, $\bar{\tau}_s$ and $\bar{\tau}_\epsilon$, are defined as

$$\bar{\tau}_s = \frac{1}{(2\pi)^2} \int_0^{2\pi} \int_0^{2\pi} \tau_s \, d\phi_0 \, d\lambda, \qquad (3)$$

$$\bar{\tau}_\epsilon = \frac{1}{(2\pi)^2} \int_0^{2\pi} \int_0^{2\pi} \tau_\epsilon \, d\phi_0 \, d\lambda, \qquad (4)$$

where ϕ_0 is the body's rotation angle and λ is the mean orbital longitude of the small body presumed here to be orbiting around the Sun in a fixed circular orbit.[3]

Nesvorný & Vokrouhlický (2007; hereafter NV07) developed an analytic theory for $\bar{\tau}_s$.[4] Here we focus on calculating $\bar{\tau}_\epsilon$. As in NV07, we assume that the studied object has a near-spherical shape. This approximation allows us to conduct all calculations analytically.

Our approach to calculating YORP torques differs in several aspects from that recently developed by Scheeres (2007; hereafter S07). In S07, the surface of the small body was defined by small triangular facets. This representation can account for

---

[3] The results can be generalized to an eccentric orbit using the method described in Section 6 of Nesvorný & Vokrouhlický (2007).

[4] Slawek Breiter alerted us to an error in Equation (B35) in NV07. This error stems from incorrect coefficients in Equations (B32) and (B33). The correct expressions for Equations (B32), (B33), and (B35) in NV07 are

$$\Delta_{k,0}^{(n)}(\alpha_2) = \frac{(n-k)!}{n!} P_n^k(\cos \alpha_2),$$

$$\Delta_{0,j}^{(n)}(\alpha_2) = (-1)^j \frac{n!}{(n+j)!} P_n^j(\cos \alpha_2),$$

and

$$J_{n,j}^{(0)} = K_{n,0}^{(0)} D_{0,j}^{(n)}\left(\frac{\pi}{2}, \frac{\pi}{2}, \frac{\pi}{2}\right) = (-1)^j \sqrt{\frac{(n-j)!}{(n+j)!}} K_{n,0}^{(0)} P_n^j(0).$$

The error does not effect the rest of Appendix B3 in NV07.

more general surface shapes than those considered here (see Section 2.2). In S07, each triangular facet was treated independently and the total radiation torque was obtained as the sum over all, typically $\sim 10^3$ to $\sim 10^6$ surface facets. This is convenient for a precise calculation of torques in a computer code. In NV07 and the present paper, we aimed at developing a theory in which the YORP torques are more tightly linked to the overall shape. This was achieved by representing the surface as series in spherical harmonics and giving analytic solutions to integrals in Equations (1), (3), and (4). The resulting expressions for the YORP torques are given as series in shape coefficients with explicit dependence of each appearing term on ϵ. This provides an important framework for our understanding of the YORP effect. Our method, however, cannot be used to precisely determine the YORP torques for elongated and/or highly-irregular bodies. Therefore, S07 and our methods are complementary.

In Section 2, we introduce several reference frames that are useful in developing the theory and use spherical harmonics to define the surface shape. In Section 3, we deal with the case where it is assumed that the surface thermal conductivity $K = 0$. The surface temperature in Equation (1) is then set by the instantaneous balance of absorbed and emitted energy fluxes which helps us to simplify calculations. General properties of $\bar{\tau}_\epsilon$ for $K = 0$ are discussed in Section 4. In Section 5, we extend the results to the case with $K \neq 0$. We do so by using a linearized heat transport equation which allows us to describe the heat conducted within the object's interior and its delayed re-emission in thermal wavelengths. We derive an approximate expression for $\bar{\tau}_\epsilon$ as a function of K. In Section 6, we apply the theory to the asteroids 1998 KY$_{26}$ and (66391) 1999 KW$_4$.

2. PRELIMINARIES

2.1. Reference Frames

To determine $\bar{\tau}_\epsilon$ we use several reference frames all with the origin at the center of mass of the small object (NV07). The body frame, $Oxyz$, has the z axis fixed along the spin axis of the body (assumed here to be aligned with the axis of maximum inertia) and the x axis along its axis of minimum inertia. The colatitude and longitude in the body frame are denoted by θ and ϕ. The rotating orbital frame, $Ox'y'z'$, has the z' axis pointing toward the normal of the orbital plane and the x' axis toward the Sun. The transformation of a vector from the rotating orbital frame to the body frame is given by

$$V = R_3(\alpha_3)R_1(\alpha_2)R_3(\alpha_1)V' \qquad (5)$$

with Euler angles $\alpha_1 = -\lambda$, $\alpha_2 = \epsilon$, and $\alpha_3 = \phi_0$, where $\phi_0 = \omega t$ denotes the phase angle of the body's rotation with respect to the inertial frame and ω is the angular frequency of rotation, ϵ is the obliquity, and λ is the mean longitude of the Sun. The symbols R_1 and R_3 in Equation (5) are the usual rotation matrices that represent the rotation of the reference system around the (generic) x and z axes, respectively. The colatitude and longitude in the rotating orbital frame are denoted by θ' and ϕ'.

Our third reference system is the frame with the z axis pointing toward the Sun and the x axis pointing toward the normal of the orbital frame. We call this reference system the solar frame. This frame rotates in an inertial system with angular speed given by the orbital motion of the small body around the Sun. The solar and rotating orbit frames are related via a sequence of three rotations by $\pi/2$ around the z, x, and z axes.

The transformation of vector V from the solar frame to the rotating orbital frame is therefore

$$V' = R_3(\alpha_3)R_1(\alpha_2)R_3(\alpha_1)V'', \qquad (6)$$

with Euler angles $\alpha_1 = \alpha_2 = \alpha_3 = \pi/2$.

2.2. Surface Shape

As in NV07, we use spherical harmonics Y_n^k to define the surface shape. This surface representation is appropriate for all shapes except those for which radial ray (θ, ϕ) can intersect the surface in more than one point. In general, the radial distance of the surface element dS from an arbitrary point inside the body can be given by

$$r(\theta, \phi) = \sum_{n \geqslant 0} \sum_{k=-n}^{n} a_{n,k} Y_n^k(\theta, \phi), \qquad (7)$$

where

$$Y_n^k(\theta, \phi) = \kappa_{n,k} P_n^k(\cos\theta)\, e^{\iota k\phi} \qquad (8)$$

and

$$\kappa_{n,k} = \sqrt{\frac{2n+1}{4\pi}\frac{(n-k)!}{(n+k)!}}. \qquad (9)$$

Here, P_n^k are the associated Legendre functions of order n and degree k, $\iota = \sqrt{-1}$ and $a_{n,-k} = (-1)^k a_{n,k}^*$, where the asterisk denotes the complex conjugate.

In the following, we will denote $r_0 = a_{0,0}/\sqrt{4\pi}$ and assume that all coefficients $A_{n,k} = a_{n,k}/r_0$ with $n \geqslant 0$ are small. Specifically, we will assume that $\varepsilon = \max(A_{n,k})_{n \geqslant 1} \ll 1$, where ε is a small parameter of the problem. This means that we limit the variety of shapes to those that can be obtained by small deformations of a sphere. Let $r = r_0(1 + \varepsilon R)$ where $\varepsilon R = \sum_{n \geqslant 1} \sum_k A_{n,k} Y_n^k(\theta, \phi)$ describes the deviation of the shape from a simple sphere. The derivatives of R with respect to angular variables will be denoted $R_\phi = \partial R/\partial\phi$ and $R_\theta = \partial R/\partial\theta$.

3. THEORY FOR $K = 0$

For $K = 0$ the surface temperature of an illuminated surface element can be calculated by equaling the absorbed and emitted energy fluxes: $\varepsilon_t \sigma T_s^4 = (1 - A)\Phi(\mathbf{n} \cdot \mathbf{n}_0)$, where A is the albedo (assumed here to be constant over the surface) and Φ is the solar flux at the orbital location of the object. Specifically, $\Phi = \Phi_{1AU} h^{-2}$, where $\Phi_{1AU} = 1378$ W m^{-2} is the solar flux at distance 1 AU from the Sun and h is the heliocentric distance of the object in AU. Vector $\mathbf{n}_0$ is the unit vector pointing from surface element dS toward the Sun. The thermal YORP torque (Equation (1)) on an object with $K = 0$ is then

$$\boldsymbol{\tau} = -\frac{2}{3}\frac{(1-A)}{v_c}\Phi \int_S dS(\mathbf{r} \times \mathbf{n})(\mathbf{n} \cdot \mathbf{n}_0), \qquad (10)$$

where the above integral is taken over the illuminated part of the surface.

The expression for torque τ_ϵ in Equation (2) has two parts. The first part $(\boldsymbol{\tau} \cdot \mathbf{s})\cos\epsilon = \tau_s \cos\epsilon$, where τ_s has been calculated in NV07. The second part, $\boldsymbol{\tau} \cdot \mathbf{o}$, can be most easily evaluated in the rotating orbital frame where $\boldsymbol{\tau} \cdot \mathbf{o} = \tau_z'$, with τ_z' being the z component of the torque in the rotating orbital frame. We have

$$\tau_z' \simeq -\alpha \int_{\Omega'} \frac{d\Omega'}{\sin\theta'}(\mathbf{r}' \times \mathbf{N}')_z I_1(\theta', \phi'), \qquad (11)$$

where $\alpha = 2\Phi(1-A)/(3v_c), d\Omega' = \sin\theta' d\theta' d\phi', \boldsymbol{N}' = \boldsymbol{t}'_\theta \times \boldsymbol{t}'_\phi$, and $\boldsymbol{t}'_\theta = \partial\boldsymbol{r}'/\partial\theta'$, and $\boldsymbol{t}'_\phi = \partial\boldsymbol{r}'/\partial\phi'$ are tangential vectors. The integration over solid angle Ω' now goes over 4π. The index z denotes the z component of the vectorial product in the rotating orbital frame.

The function I_1 in (11) is the first-order correction in ε of the insolation function of an ideal sphere. We neglect the insolation term of order zero in ε (I_0; corresponding to the insolation of an ideal sphere) because it does not contribute to the YORP torque (NV07).[5] We also neglect insolation terms $\mathcal{O}(\varepsilon^2)$ because their contribution to $\bar{\tau}_\epsilon$ is small for small shape deformations.

The term I_1 in Equation (11) can be written in spherical coordinates in the rotating orbital frame. From NV07 we have

$$I_1 = \sum_{n \geqslant 0} \sum_{k=-n}^{n} J_{n,k}^{(1)} Y_n^k(\theta', \phi'), \tag{12}$$

where

$$J_{n,k}^{(1)} = \sum_{l=-n}^{n} K_{n,l}^{(1)} D_{l,k}^{(n)}\left(\frac{\pi}{2}, \frac{\pi}{2}, \frac{\pi}{2}\right) \tag{13}$$

and

$$K_{n,l}^{(1)} = \frac{1}{r_0} \sum_{m \geqslant \max(1,|l|)} L_{n,m}^{(l)} a_{m,l}^{(S)}. \tag{14}$$

Above, $D_{l,k}^{(n)}$ are the Wigner matrices, $L_{n,m}^{(l)}$ are real coefficients and $a_{m,l}^{(S)}$ are the shape coefficients in the solar frame. See NV07 for the definition of these parameters. Specifically, the shape coefficients in the solar frame, $a_{m,l}^{(S)}$, are related to the original shape coefficients in the body frame, $a_{n,k}$ (Equation (7)), via

$$a_{m,l}^{(S)} = \sum_{p=-m}^{m} D_{p,l}^{(m)}\left(-\frac{\pi}{2}, -\frac{\pi}{2}, -\frac{\pi}{2}\right)$$
$$\times \sum_{q=-m}^{m} a_{m,q} D_{q,p}^{(m)}(-\phi_0, -\epsilon, \lambda), \tag{15}$$

where we used the transformation rules for spherical harmonics to transform (7) from the body frame to the solar frame (e.g., Giacaglia 1980; Šidlichovský 1983). Similarly, the shape in the rotating orbital frame is defined by

$$r'(\theta', \phi') = r_0(1 + \varepsilon R') = \sum_{n \geqslant 0} \sum_{k=-n}^{n} a_{n,k}^{(O)} Y_n^k(\theta', \phi'), \tag{16}$$

where the coefficients $a_{n,k}^{(O)}$ can be determined from the original ones, $a_{n,k}$ (Equation (7)), using

$$a_{n,k}^{(O)} = \sum_{j=-n}^{n} a_{n,j} D_{j,k}^{(n)}(-\phi_0, -\epsilon, \lambda). \tag{17}$$

Retaining only the lowest-order terms in ε we obtain

$$(\boldsymbol{r}' \times \boldsymbol{N}')_z \approx -\varepsilon r_0^3 R'_{\phi'} \sin\theta', \tag{18}$$

where

$$\varepsilon r_0 R'_{\phi'} = \varepsilon r_0 \frac{\partial R'}{\partial\phi'} = \sum_{n \geqslant 1} \sum_{k=-n}^{n} \iota k a_{n,k}^{(O)} Y_n^k(\theta', \phi'). \tag{19}$$

We substitute (12), (18), and (19) into Equation (11) and use the orthogonality properties of spherical harmonics to calculate the integral in Equation (11) over Ω'. The resulting expression is

$$\tau'_z = -\alpha r_0^2 \sum_{n \geqslant 1} \sum_{k=-n}^{n} \iota k a_{n,k}^{(O)*} J_{n,k}^{(1)}$$
$$= 2\alpha r_0^2 \sum_{n \geqslant 1} \sum_{k=1}^{n} k\Im\left(a_{n,k}^{(O)*} J_{n,k}^{(1)}\right), \tag{20}$$

where $\Im(\cdot)$ denotes the imaginary part. We used $J_{n,-k}^{(1)} = (-1)^k J_{n,k}^{(1)*}$ above which holds because I_1 in Equation (12) must be real.

In the next step, we substitute Equations (13) and (14) into Equation (20) to obtain

$$\tau'_z = 2\alpha r_0 \sum_{n \geqslant 1} \sum_{k=-n}^{n} \sum_{l=-n}^{n} \sum_{m \geqslant \max(1,|l|)} k D_{l,k}^{(n)}\left(\frac{\pi}{2}, \frac{\pi}{2}, \frac{\pi}{2}\right)$$
$$\times L_{n,m}^{(l)} \Im\left(a_{n,k}^{(O)*} a_{m,l}^{(S)}\right). \tag{21}$$

This last expression needs to be averaged over λ and ϕ_0 as in Equation (4). The part of Equation (21) that depends on λ and ϕ_0 is $a_{n,k}^{(O)*} a_{m,l}^{(S)}$, where these shape coefficients in the rotating orbital and solar frames were determined in Equations (15) and (17). The Wigner matrices in Equations (15) and (17) can be written as

$$D_{j,k}^{(n)}(-\phi_0, -\epsilon, \lambda) = d_{j,k}^{(n)} \Delta_{j,k}^{(n)}(-\epsilon)\, e^{\iota[k(\lambda + \pi/2) - j(\phi_0 + \pi/2)]}, \tag{22}$$

where

$$d_{j,k}^{(n)} = \frac{(n-k)!}{(n-j)!} \frac{\kappa_{n,j}}{\kappa_{n,k}} \tag{23}$$

and $\Delta_{j,k}^{(n)}(-\epsilon)$ are real functions of obliquity defined in NV07. Moreover, the coefficients $D_{p,l}^{(m)}(-\pi/2, -\pi/2, -\pi/2)$ in Equation (15) are also real.

Let $\langle\cdot\rangle$ denote the average over λ and ϕ_0. Assuming that no spin–orbit resonances exist, we find that

$$\langle a_{n,k}^{(O)*} a_{m,l}^{(S)} \rangle = D_{k,l}^{(m)}\left(-\frac{\pi}{2}, -\frac{\pi}{2}, -\frac{\pi}{2}\right)$$
$$\times \sum_{j=-\min(n,m)}^{\min(n,m)} d_{j,k}^{(n)} d_{j,k}^{(m)} \Delta_{j,k}^{(n)}(\epsilon) \Delta_{j,k}^{(m)}(\epsilon) a_{n,j}^* a_{m,j}. \tag{24}$$

The mean z-component of the torque in the rotating orbital frame is, therefore,

$$\bar{\tau}'_z = 2\alpha r_0 \sum_{n \geqslant 1} \sum_{m \geqslant 1} \sum_{k=-\min(n,m)}^{\min(n,m)} k S_k^{(n,m)}(\epsilon) \Im(a_{n,k}^* a_{m,k}), \tag{25}$$

where

$$S_k^{(n,m)}(\epsilon) = \sum_{j=-\min(n,m)}^{\min(n,m)} \Delta_{k,j}^{(n)}(\epsilon) \Delta_{k,j}^{(m)}(\epsilon) R_{k,j}^{(n,m)} \tag{26}$$

---

[5] A formal analytical proof of this statement can be obtained up to $\mathcal{O}(\varepsilon^2)$ in $\bar{\tau}_\epsilon$. See NV07, Sections 4.1 and 4.2, for a similar proof for $\bar{\tau}_s$. We checked numerically that it holds to any order in ε. Here we concentrate on the main contribution of insolation to $\bar{\tau}_\epsilon$, which is provided by I_1.

where the real coefficients $R_{k,j}^{(n,m)}$ can be determined from the above expressions. Furthermore, the sums in Equation (25) can be reduced to sums with $k \geqslant 1$ and $m > n$. We find that

$$\bar{\tau}_z' = \alpha r_0 \sum_{n \geqslant 1} \sum_{m \geqslant n+2}^{(+2)} \sum_{k=1}^{n} V_k^{(n,m)}(\epsilon) \Im(a_{n,k}^* a_{m,k}), \quad (27)$$

where the sum over m goes in increments of two due to parity properties of $L_{n,m}^{(l)}$ in Equation (14). The new functions $V_k^{(n,m)}$ are

$$\frac{1}{2k} V_k^{(n,m)}(\epsilon) = S_k^{(n,m)}(\epsilon) - S_{-k}^{(n,m)}(\epsilon) - S_k^{(m,n)}(\epsilon) + S_{-k}^{(m,n)}(\epsilon). \quad (28)$$

Equation (27) has the same functional form as Equation (44) in NV07 for $\bar{\tau}_s$. These two equations have to be combined according to Equation (2) to yield the final expression for $\bar{\tau}_\epsilon$:

$$\bar{\tau}_\epsilon = \alpha r_0 \sum_{n \geqslant 1} \sum_{m \geqslant n+2}^{(+2)} \sum_{k=1}^{n} W_k^{(n,m)}(\epsilon) \Im(a_{n,k}^* a_{m,k}), \quad (29)$$

where the functions $W_k^{(n,m)}(\epsilon)$ can be expressed as polynomials of $\cos \epsilon$ and $\sin \epsilon$. Specifically, we find that

$$W_k^{(n,m)}(\epsilon) = \sin \epsilon \sum_{l=1}^{(n+m)/2} C_l (\cos \epsilon)^{2l-1}, \quad (30)$$

where we do not explicitly denote the dependence of coefficients C_l on n, m, and k. We used the Wolfram Mathematica program to tabulate coefficients C_l. Their numerical values for $m \leqslant 7$ are given in Table 1.[6]

The series in Equation (30) does not have good convergence properties for large n and/or m. An alternative representation of $W_k^{(n,m)}(\epsilon)$ with better convergence properties can be obtained. This representation uses series in the Legendre polynomials. Specifically, we find that

$$W_k^{(n,m)}(\epsilon) = \sin \epsilon \sum_{l=1}^{(n+m)/2} A_l P_{2l-1}(\cos \epsilon). \quad (31)$$

The leading term in this series is $\propto \sin \epsilon P_{m-n-1}(\cos \epsilon)$.

For completeness we also give the corresponding expression for $\bar{\tau}_s$. From Equation (44) in NV07 we have that

$$\bar{\tau}_s = \alpha r_0 \sum_{n \geqslant 1} \sum_{m \geqslant n+2}^{(+2)} \sum_{k=1}^{n} T_k^{(n,m)}(\epsilon) \Im(a_{n,k}^* a_{m,k}). \quad (32)$$

The new representation of $T_k^{(n,m)}(\epsilon)$ in series of Legendre polynomials is

$$T_k^{(n,m)}(\epsilon) = \sum_{l=l_0}^{(n+m)/2} B_l P_{2l}(\cos \epsilon), \quad (33)$$

where $l_0 = y \equiv (m-n)/2$ is the YORP order defined in NV07. The coefficients B_l tend to zero with increasing l. Therefore, the leading term in this series is $\propto P_{m-n}(\cos \epsilon)$.

---

[6] A more complete version of this table can be found at http://www.boulder.swri.edu/~davidn/yorp_teps.txt.

Table 1
The Numerical Values of Coefficients C_l, as Defined by Equation (30), for $m \leqslant 7$

n	m	k	C_1	C_2	C_3	C_4	C_5	C_6
1	3	1	0.767	0.548				
1	5	1	−0.361	−0.266	1.996			
1	7	1	0.249	0.185	−5.746	6.862		
2	4	1	0.973	0.691	1.099			
2	4	2	1.798	1.288	−0.777			
2	6	1	−0.330	−0.242	−1.410	5.075		
2	6	2	−0.795	−0.587	6.951	−4.012		
3	5	1	1.335	0.950	−0.475	2.626		
3	5	2	2.319	1.650	3.132	−2.511		
3	5	3	3.004	2.155	−2.849	0.942		
3	7	1	−0.484	−0.356	4.180	−11.868	13.729	
3	7	2	−0.775	−0.569	−4.413	23.476	−14.179	
3	7	3	−1.270	−0.938	15.938	−18.262	6.140	
4	6	1	1.606	1.140	2.381	−5.819	6.980	
4	6	2	3.067	2.183	−1.957	11.717	−7.804	
4	6	3	3.924	2.796	6.289	−10.906	4.171	
4	6	4	4.342	3.120	−6.702	4.494	−1.077	
5	7	1	1.932	1.373	−1.378	14.773	−28.309	19.898
5	7	2	3.650	2.595	6.193	−24.467	46.703	−24.563
5	7	3	5.100	3.634	−4.889	32.942	−43.061	15.954
5	7	4	5.728	4.088	10.795	−29.734	23.075	−6.047
5	7	5	5.787	4.163	−12.812	13.038	−6.277	1.195

(This table is available in its entirety in machine-readable and Virtual Observatory (VO) forms in the online journal. A portion is shown here for guidance regarding its form and content.)

Table 2
The Functional Dependence of $\bar{\tau}_\epsilon$ and $\bar{\tau}_s$ on Obliquity ϵ for Different YORP Orders, y, and the Roots of $P_{2y}(\cos \epsilon)$ for $\epsilon < 90°$.

y	$\bar{\tau}_\epsilon / \sin \epsilon$	$\bar{\tau}_s$	Roots of $P_{2y}(\cos \epsilon)$
1	$P_1(\cos \epsilon)$	$P_2(\cos \epsilon)$	54.7°
2	$P_3(\cos \epsilon)$	$P_4(\cos \epsilon)$	30.5°, 70.1°
3	$P_5(\cos \epsilon)$	$P_6(\cos \epsilon)$	21.2°, 48.6°, 76.2°
4	$P_7(\cos \epsilon)$	$P_8(\cos \epsilon)$	16.2°, 37.2°, 58.3°, 79.4°
5	$P_9(\cos \epsilon)$	$P_{10}(\cos \epsilon)$	13.1°, 30.1°, 47.2°, 64.3°, 81.4°

Note. These roots control the obliquity values of generalized Slivan states.

4. GENERAL PROPERTIES OF $\bar{\tau}_\epsilon$ FOR $K = 0$

$W_k^{(n,m)}(\epsilon) = 0$ for $\epsilon = 0°$, $90°$, and $180°$ producing roots of $\bar{\tau}_\epsilon$ at the respective values of obliquity. Moreover, $\bar{\tau}_\epsilon(\epsilon) = -\bar{\tau}_\epsilon(\pi - \epsilon)$ because of the functional form of $W_k^{(n,m)}(\epsilon)$ in Equation (30). Adopting the classification scheme of NV07, $\bar{\tau}_\epsilon > 0$ for $0° < \epsilon < 90°$ and $\bar{\tau}_\epsilon < 0$ for $90° < \epsilon < 180°$ for Class-1 shape terms with $m = n + 2$ (Figure 1(a)). Class-2 shape terms with $m = n+2$ show opposite signs in the respective intervals (Figure 1(b)). According to Equation (30), the Class-1 behavior of shape deformations with $m = n + 2$ (YORP order 1; NV07) occurs when $\Im(a_{n,k}^* a_{m,k}) > 0$ and the Class-1 behavior occurs when $\Im(a_{n,k}^* a_{m,k}) < 0$.

To describe the behavior of YORP torques produced by deformation terms with $m > n + 2$, NV07 defined the YORP order of a deformation as $y = (m - n)/2$. Figure 2 illustrates the behavior of the Class-1 dependence of $\bar{\tau}_\epsilon$ on obliquity for $y = 2$ (panel (a)) and $y = 3$ (panel (b)). Table 2 summarizes the functional dependence of $\bar{\tau}_\epsilon$ and $\bar{\tau}_s$ on obliquity according to Equations (31) and (33).
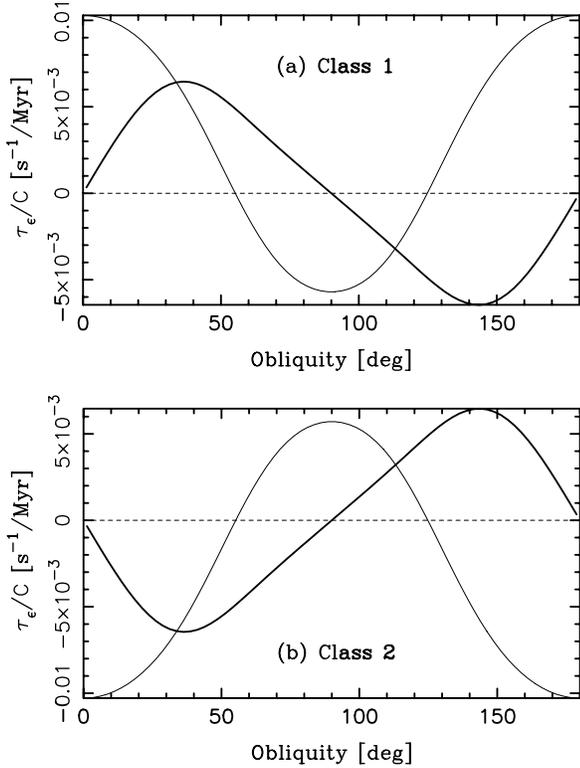
Figure 1. The two classes of YORP torques: (a) example of Class 1; (b) example of Class 2. The torque component $\bar{\tau}_\epsilon$ is denoted by the thick line. The component $\bar{\tau}_s$, denoted by the thin line, was taken from NV07. These examples correspond to a spheroidal body with radius $r_0 = 100$ m orbiting around the Sun at distance 2.5 AU. The symbol C on the ordinate denotes the principal moment of inertia of the object which we calculated assuming constant density $\rho = 2.5$ g cm^{-2}. We opted for a simple choice of shape coefficients. In both (a) and (b), we set all $a_{n,k} = 0$ except for $a_{2,0} = -10$ m to deform the sphere into a slightly oblate, axially symmetric object, and $a_{3,2} \neq 0$ and $a_{5,2} \neq 0$. In (a), we used $a_{3,2} = 10$ m and $a_{5,2} = 10\iota$ m, therefore generating a shape that leads to the Class-1 torques. In (b), we used $a_{3,2} = 10$ m and $a_{5,2} = -10\iota$ m, producing the Class-2 torques.

The main characteristic of Class-1 $\bar{\tau}_\epsilon(\epsilon)$ is that $\bar{\tau}_\epsilon > 0$ is positive in an interval $0 < \epsilon < \epsilon_0$, where the value of ϵ_0 diminishes with increasing y (cf. Figures 1, 2(a) and (b)). Also, Class 1 has $\bar{\tau}_\epsilon < 0$ in an interval near $\epsilon = \pi$. The Class-2 torques show opposite signs of $\bar{\tau}_\epsilon$ in the respective intervals. The asymptotic states of ϵ produced by $y = 1$ deformation terms are $\epsilon = 90°$ in Class 1, and $\epsilon = 0°$ and $180°$ in Class 2. Interestingly, all these asymptotic states correspond to $\bar{\tau}_s < 0$. Therefore, the theoretically expected end-state of the YORP-induced evolution is a very slow object's rotation (Vokrouhlický & Čapek 2002; Čapek & Vokrouhlický 2004).[7] The non-principal axis rotation can be triggered in such a situation (Vokrouhlický et al. 2007).

The new form of the dependence of torques on ϵ in Equations (31) and (33) gives a clear meaning to YORP order y. Specifically, torques $\bar{\tau}_\epsilon$ and $\bar{\tau}_s$ for order y are $\propto \sin\epsilon\, P_{2y-1}(\cos\epsilon)$ and $\propto P_{2y}(\cos\epsilon)$, respectively. As discussed in NV07, the roots of $\bar{\tau}_s(\epsilon)$ for $y = 1$ produce the so-called Slivan states, which arise as evolutionary end states of the asteroid spin vectors (Slivan 2002; Vokrouhlický et al. 2003). They correspond to the equilibrium points of spin-governing equations where the gravitational and YORP torques balance each other. Here we find that

---

[7] For $K \neq 0$ and/or objects for which different deformation terms set the behavior of $\bar{\tau}_\epsilon$ and $\bar{\tau}_s$, the end-state corresponding to the object's rotational spin-up may arise.
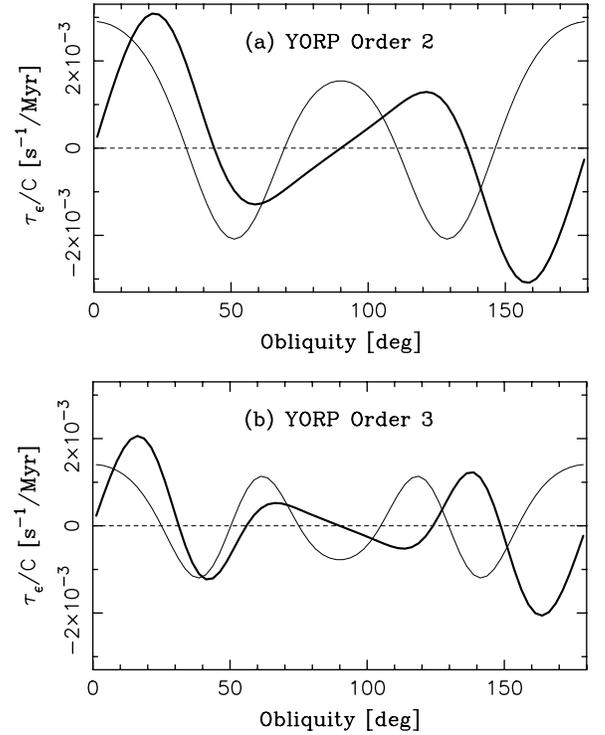
Figure 2. The illustration of Class-1 torques for YORP orders $y = 2$ (panel (a)) and $y = 3$ (panel (b)). The physical parameters and axes are the same as in Figure 1. The torque component $\bar{\tau}_\epsilon$ is denoted by the thick line. The component $\bar{\tau}_s$, denoted by the thin line, was taken from NV07. In (a), we used $a_{3,2} = 10$ m and $a_{7,2} = 10\iota$ m. In (b), we used $a_{3,2} = 10$ m and $a_{9,2} = 10\iota$ m. All other shape coefficients were set to zero except $a_{2,0} = -10$ m to deform the radius $r_0 = 100$ m sphere into a slightly oblate object.

the obliquity value of the Slivan state is given by $P_2(\cos\epsilon) = 0$ with solution $\epsilon \approx 54.7°$.

Generalized Slivan states can occur for asteroid shapes controlled by terms with $y \geqslant 2$. In these states, the obliquity will tend to values given by the solutions of $P_{2y}(\cos\epsilon) = 0$. The roots of $P_{2y}(\cos\epsilon)$ for $y \leqslant 5$ are listed in Table 2. We suggest that an important fraction of main belt asteroids may have spin states that are near (and oscillate around) these obliquity values.

For $K = 0$, a rough classification of asteroids can be achieved according to their YORP order and Class. For example, three of the four objects studied in Čapek & Vokrouhlický (2004) appear to have YORP order 1, namely 1998 KY26 (Class 1), 433 Eros (Class 1), and 243 Ida (Class 2). The fourth object studied in Čapek and Vokrouhlický, 6489 Golevka, has $\bar{\tau}_\epsilon$ of YORP order 2 and Class 2, and $\bar{\tau}_s$ that appears to have contributions from YORP orders 1 and 2. Similarly, asteroids studied in S07 show characteristics of different YORP orders and classes (e.g., 4179 Toutatis appears to have YORP order 3 and Class 2 for $K = 0$).

5. EXTENSION TO $K \neq 0$

5.1. Heat Transport Model

To determine $\bar{\tau}_\epsilon$ for $K \neq 0$ we must first compute the surface temperature which appears in Equation (1). To simplify the procedure, we will assume that certain conditions are met such that the main effects of $K \neq 0$ on torques arise from the heat transport along the surface normal into the body's interior and will neglect the heat exchange between neighbor surface elements. The heat conduction for different surface elements dS can then be treated independently. The differential equation

that describes the heat diffusion inside the object along normal n to surface element dS is

$$\rho c_P \frac{\partial T}{\partial t} = K \frac{\partial^2 T}{\partial \zeta^2}, \tag{34}$$

where ρ is the density, c_P is the specific heat capacity, and $\zeta \leqslant 0$ measures the depth along n. We assume (and show later in this section) that the insolation of the surface element dS can be expanded in Fourier series in $\phi_0 = \omega t$. Let

$$F(t) = (1 - A)\Phi \sum_k F_k \exp(\iota k \phi_0), \tag{35}$$

with $F_{-k} = F_k^*$, be the absorbed energy flux by dS. The coefficients F_k are periodic functions of λ because the insolation of dS periodically changes during the object's orbital motion around the Sun. We solve the heat conduction Equation (34) for $\lambda = $ const. This means that we neglect thermal effects in Equation (34) produced by annually varying insolation because these effects should be small compared to the (diurnal) ones produced due to the object's rotation.

The boundary conditions for $T(t, \zeta)$ are set by the following equations:

$$\varepsilon_t \sigma T^4(t, 0) + K \left(\frac{\partial T}{\partial \zeta} \right)_{\zeta=0} = F(t), \tag{36}$$

$$T(t, -\infty) = \text{const.} \tag{37}$$

These boundary conditions assure that (i) $F(t)$ is appropriately distributed between the flux radiated from dS in thermal wavelengths (the first term on the left-hand side of Equation (36)) and the heat conducted into the interior of the object (the second term in Equation (36)), and (ii) the temperature is constant at large depth. In addition, given the form of $F(t)$ in Equation (35), we assume that T is periodic in time.

We assume in the following that $T = T_0 + \Delta T$ with constant $T_0 = [((1-A)\Phi F_0)/\varepsilon_t \sigma]^{1/4}$ and $\Delta T \ll T_0$ defining the periodic temperature changes that arise from varying insolation during the object's rotation. Equations (34) and (36) can then be linearized to yield

$$\frac{\partial \Delta T}{\partial t} = \chi \frac{\partial^2 \Delta T}{\partial \zeta^2}, \tag{38}$$

$$4\varepsilon_t \sigma T_0^3 \Delta T_s + K \left(\frac{\partial T}{\partial \zeta} \right)_{\zeta=0} = (1 - A)\Phi \sum_{k \neq 0} F_k \exp(\iota k \phi_0), \tag{39}$$

where we denoted $\Delta T_s = \Delta T(t, 0)$ and $\chi = K/\rho c_P$. The solution of Equations (38) and (39) can be obtained by separating the functional dependence on spatial and time variables, and by treating individual Fourier terms in ϕ_0 independently. Specifically, we write

$$\Delta T(t, \zeta) = \sum_k a_k(\zeta) \exp(\iota k \phi_0), \tag{40}$$

and determine the amplitudes $a_k(\zeta)$ from the decoupled linear equations resulting from Equation (38). This leads to (see, e.g., Bertotti et al. 2003)

$$a_k(\zeta) = b_k \exp\left((1 + \iota)\sqrt{\frac{|k|\omega}{2\chi}} \zeta\right), \tag{41}$$

where the coefficients b_k can be obtained from Equation (39). The surface temperature is then

$$\Delta T_s(t) = \frac{(1 - A)\Phi}{4\varepsilon_t \sigma T_0^3} \sum_{k \neq 0} F_k \Psi_k \, e^{\iota(k\phi_0 - \Delta\phi_k)} \tag{42}$$

and

$$\Delta\phi_k = \text{sgn}(k) \arctan \frac{\Theta_k}{1 + \Theta_k}, \tag{43}$$

$$\Psi_k = \left(1 + 2\Theta_k + 2\Theta_k^2\right)^{-\frac{1}{2}}, \tag{44}$$

$$\Theta_k = \frac{\rho c_P}{4\varepsilon_t \sigma T_0^3} \sqrt{\frac{|k|\chi\omega}{2}}. \tag{45}$$

The thermal parameter Θ_1 is the ratio of the thermal relaxation time, required for the accumulation of the absorbed energy and its re-emission, to the rotation period (Farinella et al. 1998). The parameter $\Delta\phi_k$ is the phase lag produced by delayed emission of photons. Note that $\Delta\phi_k$ is larger for larger k (i.e., for larger frequencies) but $|\Delta\phi_k| < 45°$ for any k in the linearized theory, as can be seen from Equation (43). With formal definition $\Delta\phi_0 = 0$ and $\Psi_0 = 1$ we end up obtaining

$$T_s^4 \simeq T_0^4 + 4T_0^3 \Delta T_s$$
$$= \frac{(1 - A)\Phi}{\varepsilon_t \sigma} \sum_k F_k \Psi_k \, e^{\iota(k\phi_0 - \Delta\phi_k)}, \tag{46}$$

where the sum over k now also includes terms with $k = 0$. The term T_s^4 should be inserted into Equation (1).

The remaining piece of calculation, anticipated by Equation (35), is to show that the insolation of the surface element dS can be expanded in Fourier series in ϕ_0. Using expressions derived in Appendix B3 of NV07, we find that the absorbed flux can be written as

$$F(t) \simeq (1 - A)\Phi(I_0 + I_1)$$
$$= (1 - A)\Phi \sum_{n \geqslant 0} \sum_{k=-n}^{n} Y_n^k(\theta, \phi) \sum_q f_{k,q}^{(n)} e^{\iota(k-q)\phi_0}, \tag{47}$$

where I_0 and I_1 are the insolation terms of order zero and one in the small deformation parameter ε, respectively. We neglected terms $\mathcal{O}(\varepsilon^2)$ in the above equation. The explicit expression for $f_{k,q}^{(n)} = f_{k,q}^{(n)}(\lambda; \epsilon)$ are given in Appendix B3 in NV07. Equation (47) is the required Fourier expansion.

5.2. Torques for $K \neq 0$

Let us now return to the case considered in Section 3, where we assumed that $K = 0$. This will be helpful to appreciate the effect of K on different torque components. With Equation (47) and $K = 0$, the expression for the torque (Equation (1)) averaged over ϕ_0 retains only the terms with $q = k$. Therefore, we find for $K = 0$ that

$$\langle \tau \rangle_{\phi_0} = -\alpha \sum_{n \geqslant 0} \sum_{k=-n}^{n} f_{k,k}^{(n)} \int_S dS(r \times n) Y_n^k(\theta, \phi). \tag{48}$$

In NV07, we additionally averaged $\langle \tau \rangle_{\phi_0}$ over λ and found an explicit expression for $\bar{\tau}_s$ ($= \bar{\tau}_z$) in the $K = 0$ case.

Now we compare Equation (48) with the torque produced with $K \neq 0$. Combining Equations (46) and (47) the temperature term in Equation (1) becomes

$$T_s^4 = \frac{(1-A)\Phi}{\varepsilon_t \sigma} \sum_{n \geqslant 0} \sum_{k=-n}^{n} Y_n^k(\theta, \phi)$$
$$\times \sum_q f_{k,q}^{(n)} \Psi_{k-q} \, e^{\iota[(k-q)\phi_0 - \Delta\phi_{k-q}]}. \quad (49)$$

We insert this expression into Equation (1) and find that

$$\boldsymbol{\tau} = -\alpha \sum_{n \geqslant 0} \sum_{k=-n}^{n} \sum_q f_{k,q}^{(n)}$$
$$\times \int_S dS (\boldsymbol{r} \times \boldsymbol{n}) Y_n^k(\theta, \phi) \Psi_{k-q} \, e^{\iota[(k-q)\phi_0 - \Delta\phi_{k-q}]}. \quad (50)$$

When averaged over ϕ_0, the above expression retains only the terms with $q = k$ and we recover the original functional form of the torque in the case with $K = 0$ (Equation (48)). This shows that $\bar{\tau}_s$ is insensitive to the object's thermal conductivity properties, as was previously demonstrated numerically in Čapek & Vokrouhlický (2004) and using a different, but general approach in S07.

This result can be also explained by the following intuitive argument. Consider the thermal emission from the surface element dS which is heated by sunlight. With $K = 0$, the peak of thermal emission occurs when the Sun is seen highest above the horizon of dS (i.e., at local noon). With $K \neq 0$, the peak emission will be delayed by Δt. This time lag will lead to the situation where the temperature of dS peaks sometime in the afternoon. The thermal photon emission from dS will therefore be also delayed. Note, however, that the direction of photon emission from dS with respect to the body frame is fixed and independent of Δt. Moreover, the total energy emitted from dS over one rotation period is equal to the total absorbed energy by dS and is therefore also independent of K. This shows that τ_s, when averaged over the rotation period, is independent of K, as we rigorously demonstrated above (unless important shadowing effects occur).

We now examine the effects of K on τ_ϵ. Equation (2) can be written as

$$\tau_\epsilon = -\frac{1}{\sin\epsilon} (\tau_x o_x + \tau_y o_y), \quad (51)$$

where τ_x, τ_y and o_x, o_y are the components of the torque and orbit vectors in the body frame, respectively. We find that $(o_x, o_y) = \sin\epsilon(\sin\phi_0, \cos\phi_0)$. Using complex notation $\tau_w = \tau_x + \iota\tau_y$, the obliquity component of the YORP torque becomes

$$\tau_\epsilon = -\Im(\tau_w \, e^{\iota\phi_0}). \quad (52)$$

Before dealing with $K \neq 0$ we first consider the case with $K = 0$ because the procedure used here differs from that used in Section 3. Specifically, we perform calculations in the body frame here, while we used the rotating orbital frame in Section 3. With $K = 0$, the averaging over ϕ_0 results in

$$\langle \tau_w \, e^{\iota\phi_0} \rangle_{\phi_0} = -\alpha \sum_{n \geqslant 0} \sum_{k=-n}^{n} f_{k,k+1}^{(n)} \int_S dS (\boldsymbol{r} \times \boldsymbol{n})_w Y_n^k(\theta, \phi), \quad (53)$$

where

$$(\boldsymbol{r} \times \boldsymbol{n})_w = r_0^3 \, e^{\iota\phi} (R_\phi \cos\theta - \iota R_\theta \sin\phi). \quad (54)$$

In Section 3, we additionally averaged the torque over λ and found a closed expression for $\bar{\tau}_\epsilon$ (Equation (29)).

Returning now to the $K \neq 0$ case, we find from Equation (50) that

$$\tau_w \, e^{\iota\phi_0} = -\alpha \sum_{n \geqslant 0} \sum_{k=-n}^{n} \sum_q f_{k,q}^{(n)}$$
$$\times \int_S dS (\boldsymbol{r} \times \boldsymbol{n})_w Y_n^k(\theta, \phi) \Psi_{k-q} \, e^{\iota[(k-q+1)\phi_0 - \Delta\phi_{k-q}]}. \quad (55)$$

Averaging this over ϕ_0, we find that the expression retains only the terms with $q = k + 1$:

$$\langle \tau_w \, e^{\iota\phi_0} \rangle_{\phi_0} = -\alpha \sum_{n \geqslant 0} \sum_{k=-n}^{n} f_{k,k+1}^{(n)} \int_S dS (\boldsymbol{r} \times \boldsymbol{n})_w Y_n^k(\theta, \phi) \Psi \, e^{\iota\Delta\phi}, \quad (56)$$

where we denoted $\Psi = \Psi_1 = \Psi_{-1}$ and $\Delta\phi = \Delta\phi_1 = -\Delta\phi_{-1}$.

We assume in the following that $T_0 = T_{\rm eff} = {\rm const.}$, where $T_{\rm eff}$ is an effective temperature of a spherical body. Specifically, we set $T_{\rm eff} = [((1-A)\Phi)/\varepsilon_t \sigma]^{1/4}$ (see, e.g., Vokrouhlický 1998). The term $\Psi \exp(\iota\Delta\phi)$ can then be moved out of the integral. We end up with

$$\langle \tau_w \, e^{\iota\phi_0} \rangle_{\phi_0} \simeq -\alpha\Psi \, e^{\iota\Delta\phi} \sum_{n \geqslant 0} \sum_{k=-n}^{n} f_{k,k+1}^{(n)} \int_S dS (\boldsymbol{r} \times \boldsymbol{n})_w Y_n^k(\theta, \phi). \quad (57)$$

Comparing this to Equation (53), we see that the resulting expression for $K \neq 0$ is the same as the original expression for τ_ϵ with $K = 0$ except for the multiplication factor $\Psi \exp(\iota\Delta\phi)$ that reduces the torque's strength because $\Psi < 1$. Unlike $\bar{\tau}_s$, the torque $\bar{\tau}_\epsilon$ therefore depends on thermal conductivity which explains the finding of Čapek & Vokrouhlický (2004). Equation (29), modified to include cases with $K \neq 0$, reads

$$\bar{\tau}_\epsilon = \alpha r_0 \Psi \sum_{n \geqslant 1} \sum_{m \geqslant n+2}^{(+2)} \sum_{k=1}^{n} W_k^{(n,m)}(\epsilon)$$
$$\times [\Im(a_{n,k}^* a_{m,k}) \cos\Delta\phi + \Re(a_{n,k}^* a_{m,k}) \sin\Delta\phi], \quad (58)$$

where W_k, $\Delta\phi = \Delta\phi_1$, and $\Psi = \Psi_1$ were defined by Equations (30), (43), and (44), respectively. Note that the magnitude of the term Ψ drops with increasing K, therefore producing smaller $\bar{\tau}_\epsilon$ for larger thermal conductivities. Equation (58) is related to Equation (148) in S07. In fact, it can be inferred from the analysis in S07 that the contribution of $\Re(a_{n,k}^* a_{m,k})$ can have a very significant effect for $K \neq 0$. We will illustrate this in more detail in Section 6.

Equation (58) shows how $\bar{\tau}_\epsilon$ scales with various physical and dynamical parameters such as the surface thermal conductivity K and spin rate ω. For example, $\Psi \propto 1 - \Theta_1$ and $\Delta\phi \approx 0$ for $\Theta_1 \ll 1$, where $\Theta_1 \propto \sqrt{K\omega}$ is defined in Equation (45). Therefore, we find for small Θ_1 that $\bar{\tau}_\epsilon$ should nearly linearly diminish with increasing $\sqrt{K\omega}$. For $\Theta_1 \gg 1$, on the other hand, $\Psi \propto 1/\sqrt{K\omega}$ and $\Delta\phi \approx \pi/4$. This shows that $\Im(a_{n,k}^* a_{m,k})$ and $\Re(a_{n,k}^* a_{m,k})$ will have the same weight in $\bar{\tau}_\epsilon$ for large values of $K\omega$.

6. APPLICATION TO ASTEROIDS

The analytic theory of the YORP effect that we developed in Sections 3 and 5 can be applied to natural and artificial objects
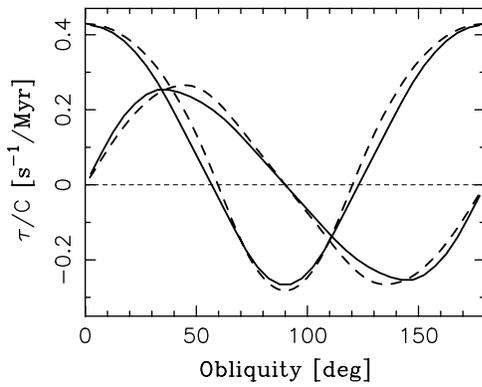
Figure 3. Thermal torques $\bar{\tau}_\epsilon$ and $\bar{\tau}_s$ for 1998 KY$_{26}$ that we determined from our analytic model (solid lines) and the exact numerical solution (dashed lines; from Čapek & Vokrouhlický 2004). Both methods used $K = 0$. The torque $\bar{\tau}_\epsilon$ is the sinusoidal-shaped curve characteristic for the YORP order 1/Class 1 deformation (compare to Figure 1(a)). The symbol C on the ordinate denotes the principal moment of inertia of 1998 KY$_{26}$ that we calculated assuming constant density, $\rho = 2.8$ g cm^{-3}. We used $a = 1.23$ AU for the semimajor axis of 1998 KY$_{26}$.

with near-spherical shapes. As an example, we discuss here results for asteroids 1998 KY$_{26}$ and (66391) 1999 KW$_4$.

6.1. 1998 KY$_{26}$

We used the shape model of 1998 KY$_{26}$ currently available on the PDS node (Ostro et al. 1999). This shape model consists of 2048 vertices that define 4092 flat surface triangles. We slightly shifted and rotated the original reference frame so that the origin almost exactly coincides with the center of mass (assuming constant density) and the z axis is nearly identical to the axis of maximum inertia of 1998 KY$_{26}$. Next, we used an interpolation routine to obtain $r(\theta, \phi)$ for any θ and ϕ and determined coefficients $a_{n,k}$ via numerical quadratures as in NV07.

The thermal YORP torque, $\bar{\tau}_\epsilon$, on 1998 KY$_{26}$ was calculated via three different methods: (1) a numerical method that uses the original polyhedral model and accounts for mutual shadowing of surface elements (Čapek & Vokrouhlický 2004); (2) a numerical method that uses the representation of shape in spherical harmonics expansion and ignores shadowing; (3) our analytic method that uses Equation (58). The results of methods (1) and (3) for $K = 0$ are shown in Figure 3. In general, there exists excellent agreement among all three methods.

According to Figure 3, the asteroid 1998 KY$_{26}$ is clearly a Class-1 object controlled by first-order YORP deformations (see Section 4 and NV07 for a definition of the YORP torque). This result can be also directly inferred from the criterion discussed in NV07, because the leading term in Equation (29), $\Im(a_{5,5}^* a_{7,5})$, is positive (4.5×10^{-8} km^2; see Table 2 in NV07). Therefore, it is indeed expected that the shape of 1998 KY$_{26}$ should produce a Class-1 YORP torque. For reference, the leading negative term is $\Im(a_{5,4}^* a_{7,4}) = -1.6 \times 10^{-8}$ km^2, about a factor of 3 smaller in magnitude than $\Im(a_{5,5}^* a_{7,5})$.

We used the method described in Section 5 to calculate $\bar{\tau}_\epsilon(\epsilon)$ for $K \neq 0$. In Figure 4 we plot the results for $K = 10^{-9}$, $10^{-8}, 10^{-7}, \ldots, 0.1, 1$, and 10 W m^{-1} K^{-1}. This figure can be compared to Figure 3 in Čapek & Vokrouhlický (2004), where $\bar{\tau}_\epsilon(\epsilon)$ was calculated for the same values of K using a numerical method. The agreement is good. Some of the slight differences apparent for large conductivity values probably stem from the approximative treatment of the heat conduction within the body that we adopted in this work.
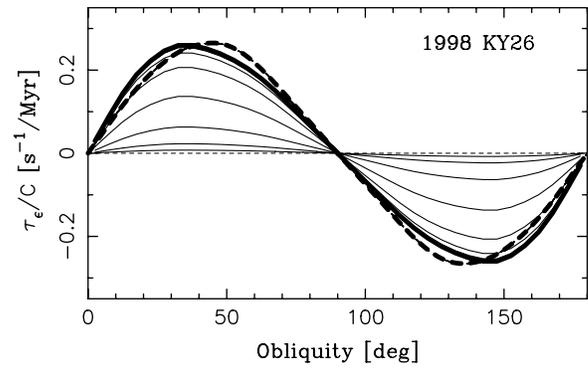
Figure 4. Effect of the thermal conductivity K on $\bar{\tau}_\epsilon$. As in Figure 3, the case with $K = 0$ is denoted by the thick solid line. Cases corresponding to K ranging from 10^{-9} to 1 W m^{-1} K^{-1} are denoted by the thin solid lines. For reference, the dashed line shows the exact numerical solution for $K = 0$. This figure can be compared with Figure 3 in Čapek & Vokrouhlický (2004).
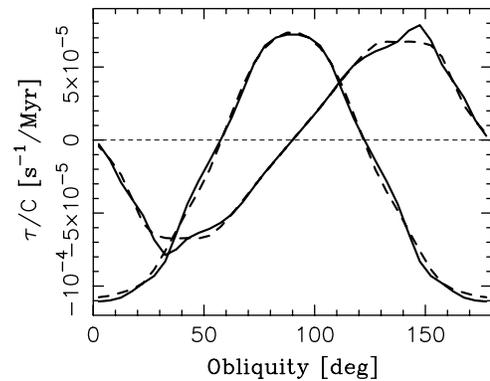
Figure 5. Thermal torques $\bar{\tau}_\epsilon$ and $\bar{\tau}_s$ for (66391) 1999 KW$_4$ that we determined from our analytic model (solid lines) and the exact numerical solution (dashed lines). Both methods used $K = 0$ and a low-resolution shape model defined by coefficients $a_{n,k}$ up to $n = 24$. Obtained torques are characteristic for the YORP order 1/Class 2 deformation (compare to Figure 1(b)). Symbol C on the ordinate denotes the principal moment of inertia of (66391) 1999 KW$_4$ that we calculated assuming constant density $\rho = 2.0$ g cm^{-3}. We used $a = 0.64$ AU for the semimajor axis of (66391) 1999 KW$_4$.

6.2. (66391) 1999 KW$_4$

The asteroid (66391) 1999 KW$_4$ is a binary system with the ≈ 1.5 km diameter primary (alpha) and ≈ 0.5 km diameter secondary (beta) components. We neglected the effect of interaction between beta on alpha and calculated thermal torques on alpha only. We used the shape model of alpha as derived from radar imaging by Ostro et al. (2006). This shape model consists of 4586 vertices. Coefficients $a_{n,k}$ up to $n = 24$ were determined for the shape model. This gives the $\approx 15°$ angular resolution of the surface features, including the alpha's prominent equatorial bulge. The bulk density $\rho = 2$ g cm^{-3} and semimajor axis $a = 0.64$ AU were assumed (Ostro et al. 2006). Below we describe the results for $K = 0$.

Figure 5 shows the torques $\bar{\tau}_\epsilon$ and $\bar{\tau}_s$ for 1999 KW$_4$. To validate our calculation we compared results obtained with methods (2) and (3) described in Section 6.1. The agreement between the numerical and analytical results is pretty good. Both show torques characteristic of the YORP order 1/Class 2 surface deformation.

When we compared these results to those recently obtained for 1999 KW$_4$ by Scheeres & Mirrahimi (2008), we found that the results differ. For example, Scheeres & Mirrahimi (2008) showed that both $\bar{\tau}_\epsilon$ and $\bar{\tau}_s$ should be positive in an interval near

$\epsilon = 0$, while we find that $\bar{\tau}_\epsilon < 0$ and $\bar{\tau}_s < 0$ near $\epsilon = 0$. This difference probably stems from the fact that we approximated the surface of 1999 KW$_4$ by spherical harmonics up to $n = 24$ only. We verified that our results become slightly more similar to those of Scheeres & Mirrahimi (2008) when the resolution is increased. We were unable, however, to push the resolution beyond $n = 36$ due to various problems with the numerical evaluation of coefficients in series in Equations (29) and (32). We will address this issue in our future work.

7. CONCLUSIONS

We developed an analytic theory for the YORP effect on obliquity. Our results show that $\bar{\tau}_\epsilon$ is sensitive to surface thermal conductivity, K. For $K \sim 0.01$–$1\,\mathrm{W\,m^{-1}\,K^{-1}}$, which may be the realistic range of conductivity values for small asteroids, torque $\bar{\tau}_\epsilon$ can be modified by a large factor relative to the $K = 0$ case. For $\Theta_1 \gg 1$, where $\Theta_1 \propto \sqrt{K\omega}$ as defined by Equation (45), $\bar{\tau}_\epsilon \propto 1/\sqrt{K\omega}$, showing that the obliquity component of the torque should diminish when a fast-rotating, small asteroid is spun up by $\bar{\tau}_s$.

Conversely, the analytic results discussed in Section 5 show that $\bar{\tau}_s$ should be nearly independent of K because it is not affected by a phase lag or diminished variation of temperature of a surface element during its rotation. Instead, these results suggest that $\bar{\tau}_s$ stems from the global surface variation of the spin-averaged temperature (due to different tilts of surface elements with respect to the annually changing sunlight).

These findings explain the behavior of YORP torques found in previous studies (Čapek & Vokrouhlický 2004, S07). They have important implications for spin dynamics of small asteroids that are subject to YORP torques.

REFERENCES

Bertotti, B., Farinella, P., & Vokrouhlický, D. 2003, Physics of the Solar System, Astrophysics and Space Science Library (Dordrecht: Kluwer), 293
Čapek, D., & Vokrouhlický, D. 2004, Icarus, 172, 526
Farinella, P., Vokrouhlický, D., & Hartmann, W. K. 1998, Icarus, 132, 378
Giacaglia, G. E. O. 1980, Stud. Geophys. Geod., 24, 1
Nesvorný, D., & Vokrouhlický, D. 2007, AJ, 134, 1750
Ostro, S. J., et al. 1999, Science, 285, 557
Ostro, S. J., et al. 2006, Science, 314, 1276
Rubincam, D. P. 2000, Icarus, 148, 2
Scheeres, D. J. 2007, Icarus, 188, 430
Scheeres, D. J., & Mirrahimi, S. 2008, Celest. Mech. Dyn. Astron., 101, 69
Šidlichovský, M. 1983, Bull. Astron. Inst. Czechosl., 34, 65
Slivan, S. M. 2002, Nature, 419, 49
Vokrouhlický, D. 1998, A&A, 338, 353
Vokrouhlický, D., & Čapek, D. 2002, Icarus, 159, 449
Vokrouhlický, D., Nesvorný, D., & Bottke, W. F. 2003, Nature, 425, 147
Vokrouhlický, D., Breiter, S., Nesvorný, D., & Bottke, W. F. 2007, Icarus, 191, 636